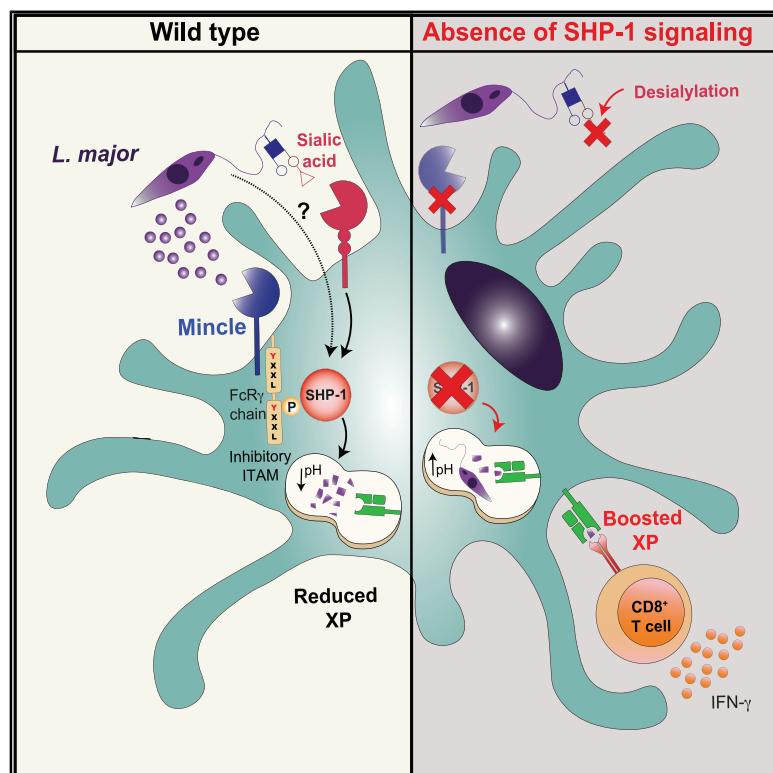


# SHP-1 Regulates Antigen Cross-Presentation and Is Exploited by *Leishmania* to Evade Immunity

## Graphical Abstract



## Authors

Sofía C. Khouili, Emma C.L. Cook, Elena Hernández-García, María Martínez-López, Ruth Conde-Garrosa, Salvador Iborra

## Correspondence

siborra@ucm.es

## In Brief

Khouili et al. identify SHP-1 as a negative regulator of antigen cross-presentation that *Leishmania* can trigger by interacting with Mincle and sialic-acid-binding receptors, dampening early CD8<sup>+</sup> T cell recognition. Loss of functional SHP-1 in CD11c<sup>+</sup> cells decreases endosomal acidification, increases cross-presentation, and boosts CD11c<sup>+</sup> cell-based vaccination against *Leishmania*.

## Highlights

- Lack of Mincle or SHP-1 loss in CD11c<sup>+</sup> cells raises CD8<sup>+</sup> T cell priming to *Leishmania*
- SHP-1 deficiency increases endosomal pH and enhances antigen cross-presentation
- SHP-1 inhibition boosts CD11c<sup>+</sup> cell-based vaccination efficacy against *Leishmania*



## Report

# SHP-1 Regulates Antigen Cross-Presentation and Is Exploited by *Leishmania* to Evade Immunity

Sofía C. Khouili,<sup>1</sup> Emma C.L. Cook,<sup>2</sup> Elena Hernández-García,<sup>2</sup> María Martínez-López,<sup>3</sup> Ruth Conde-Garroza,<sup>1</sup> and Salvador Iborra<sup>2,4,\*</sup>

<sup>1</sup>Immunobiology Lab, Centro Nacional de Investigaciones Cardiovasculares Carlos III (CNIC), 28029 Madrid, Spain

<sup>2</sup>Department of Immunology, School of Medicine, Universidad Complutense de Madrid, 12 de Octubre Health Research Institute (imas12), Madrid, Spain

<sup>3</sup>Champalimaud Research, Champalimaud Centre for the Unknown, Av. Brasília, 1400-038 Lisboa, Portugal

<sup>4</sup>Lead Contact

\*Correspondence: [siborra@ucm.es](mailto:siborra@ucm.es)

<https://doi.org/10.1016/j.celrep.2020.108468>

## SUMMARY

Intracellular pathogens have evolved strategies to evade detection by cytotoxic CD8<sup>+</sup> T lymphocytes (CTLs). Here, we ask whether *Leishmania* parasites trigger the SHP-1-FcR $\gamma$  chain inhibitory axis to dampen antigen cross-presentation in dendritic cells expressing the C-type lectin receptor Mincle. We find increased cross-priming of CTLs in *Leishmania*-infected mice deficient for Mincle or with a selective loss of SHP-1 in CD11c<sup>+</sup> cells. The latter also shows improved cross-presentation of cell-associated viral antigens. CTL activation *in vitro* reveals increased MHC class I-peptide complex expression in Mincle- or SHP-1-deficient CD11c<sup>+</sup> cells. Neuraminidase treatment also boosts cross-presentation, suggesting that *Leishmania* triggers SHP-1-associated sialic-acid-binding receptors. Mechanistically, enhanced antigen processing correlates with reduced endosomal acidification in the absence of SHP-1. Finally, we demonstrate that SHP-1 inhibition improves CD11c<sup>+</sup> cell-based vaccination against the parasite. Thus, SHP-1-mediated impairment of cross-presentation can be exploited by pathogens to evade CTLs, and SHP-1 inhibition improves CTL responses during vaccination.

## INTRODUCTION

Host immunity against intracellular pathogens is orchestrated by T helper (Th) type 1 cells and frequently requires the participation of CD8<sup>+</sup> cytotoxic T lymphocytes (CTLs). CTLs produce high amounts of proinflammatory cytokines and kill infected target cells (Schmidt and Varga, 2018). Generation of memory CTLs is an important goal of vaccination against intracellular pathogens and, potentially, tumors (Enamorado et al., 2017; Huster et al., 2006; Klebanoff et al., 2006; Wherry and Ahmed, 2004). *Leishmania* is an obligate intracellular protozoan parasite that establishes itself within the phagolysosome of host phagocytic cells, mainly macrophages. CTLs contribute to parasite control during experimental visceral leishmaniasis (VL) (Stäger and Rafati, 2012) and in cutaneous leishmaniasis (CL) induced by a low dose infection with *L. major* in mice (Belkaid et al., 2002). IFN- $\gamma$  production by CTLs blocks the development of Th2 cells, favoring the development of protective Th1 responses (Uzonna et al., 2004). CTL effector responses are lower than CD4<sup>+</sup> T cell responses in human CL (Boussoffara et al., 2019; Nateghi Rostami et al., 2010) and sometimes undetectable in VL patients (Gautam et al., 2014). Poor activation and expression of PD-1, CTLA-4, and other markers of exhausted CTL (Gautam et al., 2014; Viana et al., 2019) suggest low efficiency of *Leishmania*

antigen presentation into major histocompatibility complex (MHC) class I molecules.

Dendritic cells (DCs) initiate and control the magnitude and the quality of CTL responses because of their capacity to process peptides into MHC class I complexes, while decoding and integrating signals received from their milieu, which are then conveyed to naive CTLs (Iborra et al., 2016b; Kim et al., 2014; Zammit et al., 2005). The main mechanism providing peptides for MHC class I relies on proteasomal degradation of defective ribosomal products and other rapidly degraded proteins in the cytosol. DCs can also engulf infected cells or pathogen products, which can be translocated to the cytosol and degraded by the proteasome. In both pathways, the resulting polypeptides are delivered into the endoplasmic reticulum through the transporter associated with antigen processing (TAP), trimmed, and presented to naive CTLs. How these peptides are processed, outcompeting an overwhelming supply of constitutively generated peptides, is not well understood (see Yewdell et al., 2019, for a recent review). *Leishmania* is confined almost exclusively within phagolysosomes in macrophages, and its cross-presentation is circumscribed to an inefficient proteasome and TAP-independent phagosomal pathway (Bertholet et al., 2005, 2006), which might facilitate its transmission to other hosts (Martínez-López et al., 2018). In this line, *Leishmania*-specific CD8<sup>+</sup> T cell priming does not require Batf3-dependent DCs, which are cells



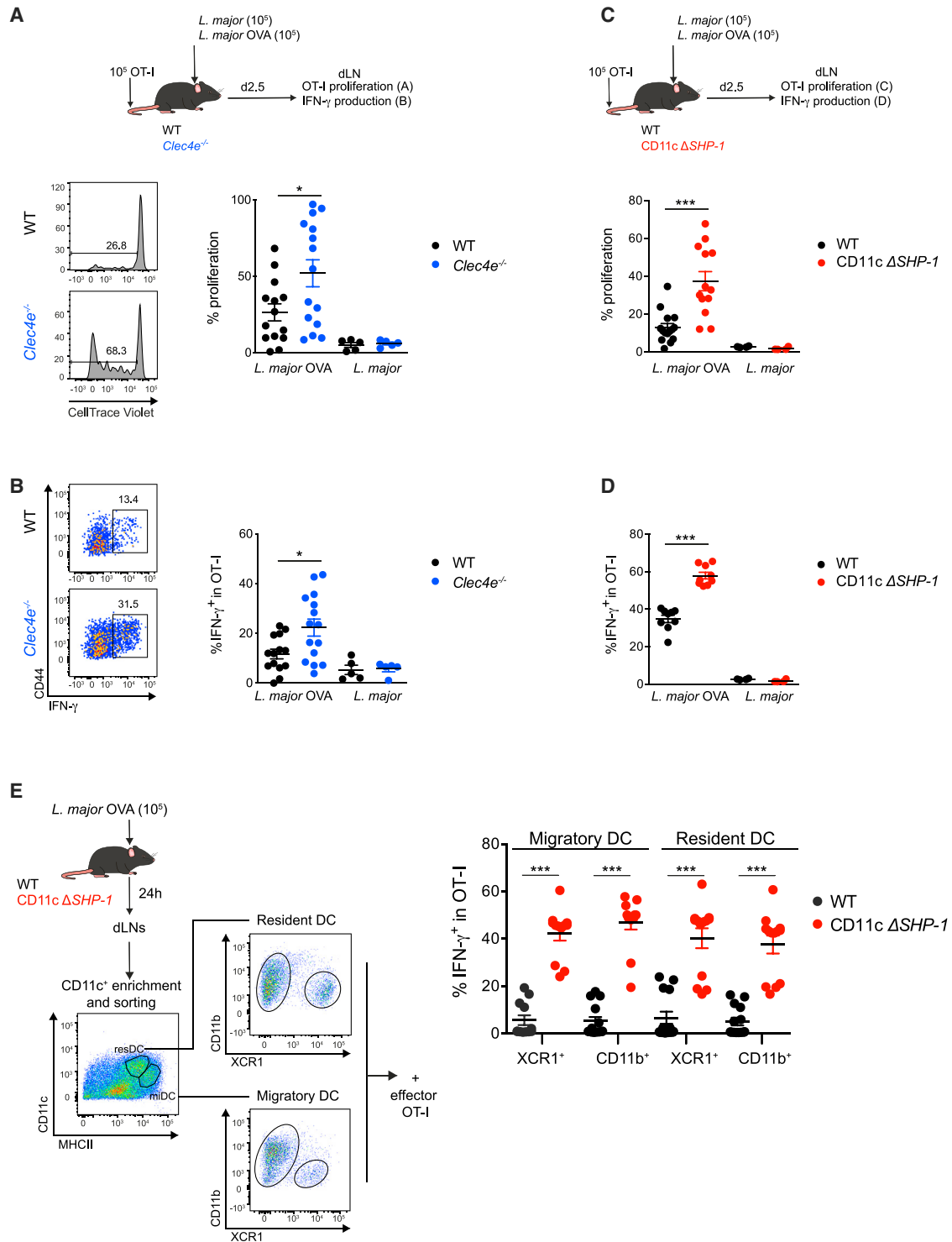


**Figure 1. Increased CD8<sup>+</sup> T Cell Priming in Mincle-Deficient and in CD11c $\Delta$ SHP-1 Mice during *L. major* Infection**

(A and B) WT and *Clec4e*<sup>-/-</sup> mice were transferred intravenously (i.v.) with CD45.1<sup>+</sup> OT-I OVA-specific CD8<sup>+</sup> T cells labeled with CellTrace Violet and infected i.d. in the ear with  $10^5$  of either *L. major* or recombinant *L. major* expressing OVA (*L. major*-OVA). (A) Left: representative histograms showing CellTrace Violet dilution in OT-I cells in draining lymph nodes (dLNs) 2.5 days post-infection (p.i.). Right: quantification of the percentage of proliferating (CellTrace Violet<sup>lo</sup>) OT-I in dLNs. (B) Left: representative plots of IFN- $\gamma$  production by OT-I following *ex vivo* restimulation of dLNs with OVA<sub>257-264</sub> peptide. Right: quantification of the percentages of IFN- $\gamma$ <sup>+</sup> OT-I in dLNs.

(legend continued on next page)

optimally equipped for cross-presentation (Martínez-López et al., 2015). Sensing of apoptotic *L. major*-infected neutrophils by Mer tyrosine kinase-dependent signaling in DCs indirectly inhibits CTL priming (Ribeiro-Gomes et al., 2015). *Leishmania* metalloprotease GP63 cleaves a subset of SNAREs, including VAMP8, preventing the assembly of the NADPH oxidase complex (NOX2). This strategy is critical to limit the acidification in cross-presentation compartments (Matheoud et al., 2013; Matte et al., 2016), preventing a complete and premature destruction of MHC class I ligands by proteases (Savina et al., 2006). Although *Leishmania* would benefit from actively inhibiting cross-presentation, we are not aware of any other strategy being described so far. Here we show that *Leishmania* dampens cross-presentation by triggering the SHP-1 inhibitory axis in DC.

## RESULTS AND DISCUSSION

The C-type lectin receptor Mincle (*Clec4e*) couples to the Fc receptor  $\gamma$  chain (FcR $\gamma$ C) that bears an immunoreceptor tyrosine-based activation motif (ITAM). A ligand released by *Leishmania* and sensed by Mincle shifts to an inhibitory ITAM configuration that recruits the protein-tyrosine phosphatase SHP-1 (PTPN6) (Iborra et al., 2016a). Mice deficient in Mincle, or lacking SHP-1 in CD11c<sup>+</sup> cells, show more robust DC activation and migration, resulting in enhanced priming of Th1 cells (Iborra et al., 2016a). Infection with *L. major* expressing chicken ovalbumin (OVA) in the ear dermis of wild-type (WT) mice induced very poor priming of OVA-specific CD8<sup>+</sup> OT-I cells in auricular draining lymph nodes (dLNs) (Figure 1A) (Martínez-López et al., 2015). OT-I T cell proliferation was significantly increased in infected *Clec4e*<sup>-/-</sup> mice *in vivo* (Figure 1A), with increased IFN- $\gamma$  production upon OVA peptide (OVA<sub>257-264</sub>) restimulation *ex vivo* (Figure 1B). We observed that this improved priming of CD8<sup>+</sup> T cells specific for *L. major*-associated antigen was phenocopied in mice lacking SHP-1 in CD11c<sup>+</sup> cells (CD11c $\Delta$ SHP-1) (Abram et al., 2013) (Figures 1C and 1D). We (and others) have shown that Mincle is not expressed by cDC1 but rather by monocyte-derived DCs and some subsets of cDC2 (Iborra et al., 2016a; Martínez-López et al., 2019) (<http://www.immgen.org>). To determine whether the SHP-1-dependent increased in CD8<sup>+</sup> T cell priming is restricted to Mincle-expressing DCs, resident and migratory DCs from auricular dLNs after *L. major*-OVA infection were sorted and separated into XCR1<sup>+</sup> (cDC1) and CD11b<sup>+</sup> (cDC2 and monocyte-derived DCs) cells and co-cultured with effector OT-I cells generated *in vitro* (Figure 1E). CTL activation, determined by intracellular staining of IFN- $\gamma$ , allows the detection of MHC class I-peptide (K<sup>b</sup>/OVA<sub>257-264</sub>) complexes (pMHC) with high sensitivity (Medina et al., 2009). Using this method, we observed that SHP-1 deletion improved the antigen cross-presentation capacity of each sorted CD11c<sup>+</sup> DC subset (Figure 1E), indicating that diverse SHP-1-dependent mecha-

nisms triggered by *Leishmania* infection might be dampening cross-presentation. In fact, several ITIM-containing inhibitory receptors (Pirb, Sirp $\alpha$ , PECAM-1, Fc $\gamma$ R1b, Clec4a2, and Clec12a) expressed by DCs recruit SHP-1 (Abram and Lowell, 2017).

These results prompted us to test whether CTL cross-priming (XP) against viral antigens from infected dead cells, which relies on Batf3-dependent cDC1 *in vivo* (Hildner et al., 2008; Iborra et al., 2012; Zelenay et al., 2012), is also affected in CD11c $\Delta$ SHP-1 mice. Following inoculation of vaccinia virus (VACV)-infected RAW macrophages (H-2<sup>d</sup>) irradiated with UV (RAW-VACV-UV) to inactivate the virus, WT mice exhibited less CD44<sup>+</sup> CTL specific for the VACV immunodominant peptide B8R<sub>20-27</sub> compared with CD11c $\Delta$ SHP-1 littermates (Figures S1A and S1B) and lower frequencies of IFN- $\gamma$ -producing CTLs upon B8R<sub>20-27</sub> restimulation (Figures S1C and S1D). Thus, SHP-1-mediated inhibition of XP affects also XP of virus-specific CTL.

Next, we asked if Mincle and SHP-1 impair CD8<sup>+</sup> T cell XP by affecting MHC class I-peptide complex formation, not by simply increasing DC maturation and migration to dLNs (Abram and Lowell, 2017; Abram et al., 2013; Iborra et al., 2016a; Kaneko et al., 2012). For that, we used effector OT-I CTLs generated *in vitro*, which only require to engage K<sup>b</sup>/OVA<sub>257-264</sub> complexes for their activation. We used CD11c<sup>+</sup> GM-CSF bone marrow-derived cells (GM-BM) from WT, *Clec4e*<sup>-/-</sup>, and CD11c $\Delta$ SHP-1 mice as antigen-presenting cells (Figure 2A), because they consist of a mix of macrophages (BM-Macs) and CD11b cDC2 (BM-DCs) (Helft et al., 2015) that either constitutively express Mincle (BM-Macs) or upon stimulation (BM-DCs) (Martínez-López et al., 2019). We observed poor cross-presentation of *Leishmania*-associated OVA antigen to effector OT-I cells in WT GM-CD11c<sup>+</sup> cells, compared with Mincle-deficient or SHP-1-deficient GM-BM (Figures 2B and 2C). As SHP-1 impairs CD8<sup>+</sup> T cell XP independently of Mincle expression (Figure 1E), we evaluated Flt3L bone marrow-derived DCs (Flt3L BMDCs), a source of cDC1 that, as aforementioned, do not express Mincle. We found that SHP-1 deficiency in Flt3L BMDCs or inhibition of SHP-1 by treatment with the SHP-1/2 phosphatase inhibitor NSC-87877 increased the cross-presentation capacity of *Leishmania*-associated OVA antigen to OT-I cells (Figure 2D). Similarly, we explored their capacity to cross-present *Leishmania* to antigen-specific memory CD8<sup>+</sup> T cells. For that, we co-cultured *Leishmania* freeze/thawed (F/T)-loaded Flt3L BMDCs with antigen-experienced cells (CD44<sup>+</sup>) CD8<sup>+</sup> T cells purified from the spleen of *Leishmania*-infected and healed mice, or CD44<sup>+</sup> cells from naive mice, and we performed polyclonal stimulation 3 days later. We observed an increased IFN- $\gamma$  production by memory CD8<sup>+</sup> T cells cultured with SHP-1-deficient DCs or NSC-87877-treated DCs, compared with WT untreated DCs (Figure 2E), without affecting bystander activation. To confirm that SHP-1 also inhibits cross-presentation of exogenous viral

(C and D) WT and CD11c $\Delta$ SHP-1 mice were transferred i.v. with CD45.1<sup>+</sup> OT-I and infected with *L. major* or *L. major*-OVA as in (A) and (B). (C) Quantification of the percentage of proliferating (CellTrace Violet<sup>+</sup>) OT-I in dLNs. (D) Quantification of the percentages of IFN- $\gamma$ <sup>+</sup> OT-I in dLNs.

(E) Effector OT-I T cells were co-cultured with migratory (MHCII<sup>hi</sup>) or resident (MHCII<sup>lo</sup>) CD11b<sup>+</sup> DCs or XCR1<sup>+</sup> DCs, sorted as indicated in the picture from the auricular dLNs from the indicated genotypes (1:1 ratio), and IFN- $\gamma$  production was quantified.

Individual data from at least two pooled experiments of three performed are shown as mean  $\pm$  SEM. \*p < 0.05, \*\*p < 0.01, and \*\*\*p < 0.001 (unpaired two-tailed Student's t test).

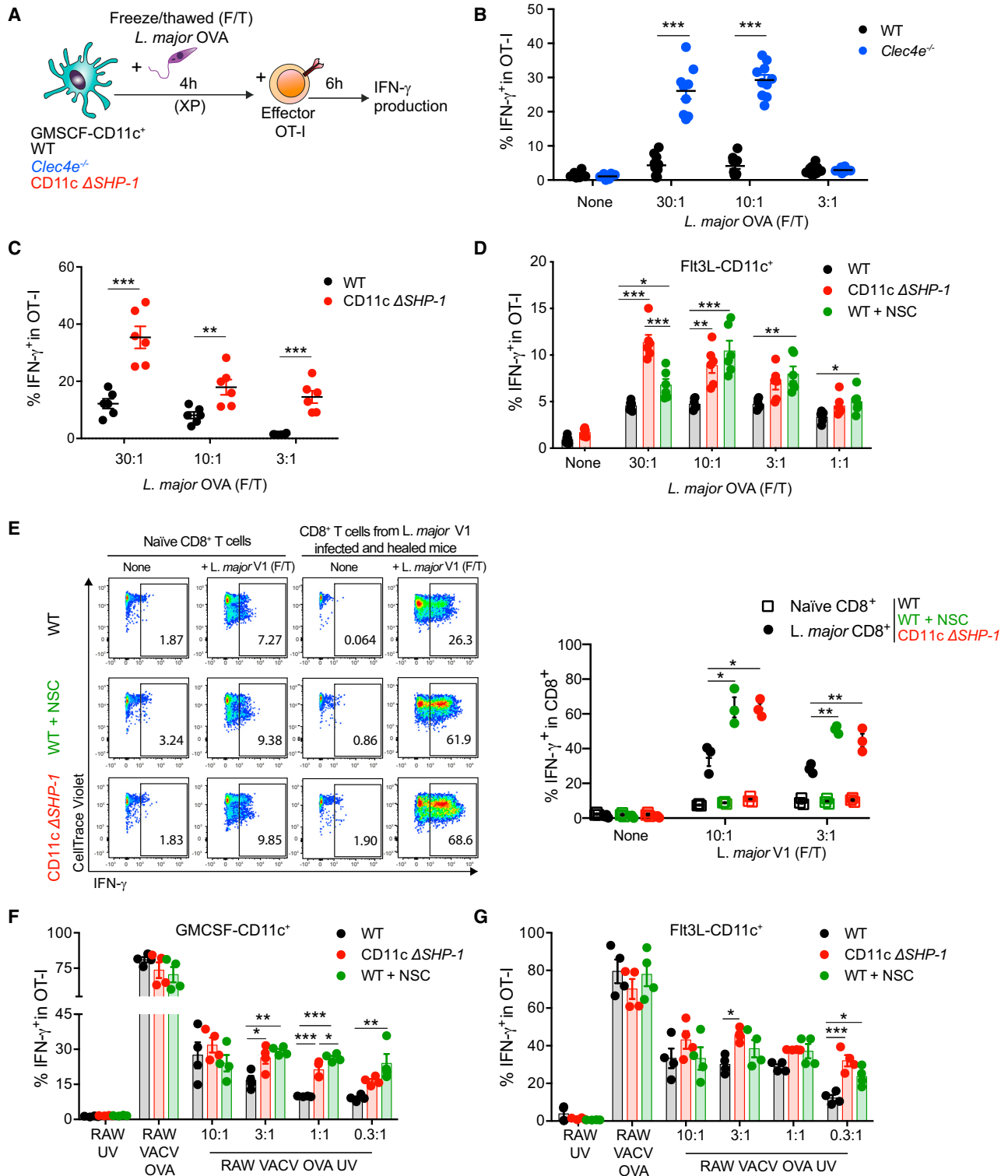


**Figure 2. Mincle or SHP-1 Deficiency in Antigen-Presenting Cells Improves Antigen Cross-Presentation**

(A) Scheme of antigen presentation assays.

(B–E) CD11c<sup>+</sup> cells purified from GM-BM (B and C) or Fit3L BMDC (D and E) of the indicated genotype were exposed for 4 h to titrated freeze/thawed (F/T) *L. major*-OVA. Cells were thereafter co-cultured for 6 h, in the presence of BFA for the last 4 h, with *in vitro* expanded OT-I T cells (B–D) or CD44<sup>+</sup> CD8<sup>+</sup> T cells from either naïve mice or *L. major*-V1 infected and healed C57BL/6 mice (E). Cultures were stained for CD8 and intracellular IFN- $\gamma$ .

(legend continued on next page)

antigens from infected dead cells, we treated GM-BM (Figure 2F) or Flt3L BMDCs (Figure 2G) with VACV-OVA-infected RAW macrophages irradiated (RAW-VACV-OVA-UV) or not (RAW-VACV-OVA) with UV. SHP-1 deficiency or inhibition with NSC-87877 increased cross-presentation of OVA<sub>257–264</sub> to effector OT-I cells both in GM-BM (Figure 2F) and Flt3L BMDCs (Figure 2G) or cross-presentation of viral antigens to effector CD8<sup>+</sup> T cells purified from VACV-infected mice (Figures S2A and S2B). Interestingly, SHP-1-deficient but not Mincle-deficient GM-BM were more efficient at cross-presenting OVA antigen coupled to latex beads, suggesting that *cis-trans* interactions of ligands with receptors triggering SHP-1 activation inhibit cross-presentation even in basal conditions (Figures S2C and S2D).

Siglec-G, a sialic-acid-binding lectin broadly expressed in DCs, inhibits cross-presentation by a mechanism that involves SHP-1 (Ding et al., 2016). We determined the role of sialic acids in the SHP-1-mediated effects on *Leishmania*-associated antigen cross-presentation. We found staining with sialic-acid-binding proteins on the surface of live and F/T *Leishmania* parasites (Figure S3A), which was prevented by sialidase (neuraminidase) treatment (Figures S3A and S3B). *Leishmania* cannot synthesize its own sialic acid and is not endowed with trans-sialidase activity. We reasoned that the parasite scavenged or acquired sialic acids from an external source (Chava et al., 2004; Roy and Mandal, 2016). In fact, recognition of sialic acids on the parasites was directly proportional to the percentage of fetal calf serum (FCS) in the culture medium (Figure S3C), while the expression of Mincle ligand by *L. major* is not affected by the presence or absence of serum (Figure S3C). We observed that the poor cross-presentation of *Leishmania*-associated OVA antigen to effector OT-I cells in WT GM-BM cells could be reverted by either pretreating the cells with NSC-87877 or treating *Leishmania* F/T extracts with sialidase (Figure 3A). Removal of sialic acids on the surface of DC might improve antigen cross-presentation (Silva et al., 2016, 2020). However, we did not find a decrease in the abundance of sialic acids on DC due to residual neuraminidase activity (Figure S3D) or an increase in IFN- $\gamma$  production by OT-I cells in the absence of cognate antigen (Figure S3E). On the other hand, both sialidase treatment and SHP-1 inhibition increased cross-presentation of *Leishmania*-associated OVA antigen in Mincle-deficient GM-BM, confirming that, besides Mincle, other receptors coupled to SHP-1 are able to dampen antigen processing (Figure 3B) and that Mincle is not involved in the recognition of sialic acids. It has been shown that Siglec-G can recruit SHP-1 to dephosphorylate p47phox, which inhibits NOX2 activation in the phagosomes of DC, consequently increasing phagosomal acidification (Ding et al., 2016). We confirmed these observations by assessing endosomal acidification using pH-sensitive or insensitive dextrans. WT or SHP-1-deficient GM-BM (Figure 3C) or Flt3L BMDCs (Figure 3D) were treated with (1) pH-insensitive Alexa 647-labeled dextrans; (2) fluorescein

isothiocyanate (FITC)-labeled dextran, whose fluorescence diminishes with acidification; and (3) pHrodo dextran, which is almost non-fluorescent at neutral pH and fluoresces brightly in acidic environments. We observed by flow cytometry that endocytosis of Alexa 647-labeled dextrans was not affected by SHP-1-deficiency in both types of antigen-presenting cells. In contrast, pHrodo fluorescence increased with incubation time, while FITC fluorescence diminished in an SHP-1-dependent manner (Figures 3C and 3D), confirming that SHP-1 promotes endosomal acidification, which might cause an increased or premature antigen degradation, preventing cross-presentation (Mantegazza et al., 2008; Savina et al., 2006).

Vaccines aimed at generating potent CTL responses largely depend on cross-presentation. Therefore, we determined if SHP-1 inhibition could specifically improve antigen cross-presentation during vaccination. For that, we cultured WT, treated or not with NSC-87877, or SHP-1-deficient GM-BM, with VACV-infected RAW macrophages irradiated with UV (RAW-VACV-UV) (as in Figure 2F), which were also loaded with an excess of influenza PR8 NP<sub>366–374</sub> peptide (Figure 4A). We inoculated mice i.v. with these GM-BM cells and assessed direct priming (DP) of NP-specific or XP of B8R-specific CD8<sup>+</sup> T cells, by using specific fluorescent labeled pMHC class I multimers (D<sup>b</sup>/NP<sub>366–374</sub> peptide or K<sup>b</sup>/B8R<sub>20–27</sub>, respectively) (Figure 4A). We found increased frequencies of B8R-specific CD8<sup>+</sup> T cells, but not of NP-specific CD8<sup>+</sup> T cells, in mice vaccinated with cells deficient for SHP-1 or treated with the inhibitor compared with WT mice (Figure 4B). We found similar results using sodium stibogluconate (SSG) to inhibit SHP-1, and GM-BM loaded with an excess of OVA<sub>257–264</sub> peptide to determine DP (Figure S4A). Therefore, we found that GM-BM-based vaccination could benefit from SHP-1 inhibition because it improves antigen cross-presentation.

We finally tested the global beneficial effects of SHP-1 inhibition during vaccination against CL in BALB/c mice, which are highly susceptible to *L. major* infection. For that, we inoculated intradermally (i.d.) into the ears GM-BM cells loaded with F/T *Leishmania*, treated or not with NSC-87877 and/or CpG ODN. Six weeks later, we infected the mice with a low dose of *L. major* in the ear, a physiological setting of CL that, as aforementioned, requires CD8<sup>+</sup> T cells for an efficient control of the parasite (Belkaid et al., 2002). We analyzed T cell responses in the ear 6 days after infection. For that, ear cell suspensions were cultured with GM-BM loaded with F/T *Leishmania* *ex vivo*. We found a higher frequency of IFN- $\gamma$ - and TNF- $\alpha$ -producing CD8<sup>+</sup> T cells (Figure 4C), and lower parasite loads (Figure 4D), in mice vaccinated with *Leishmania*-loaded GM-BM treated with NSC-87877, compared with unvaccinated mice, or mice treated with *Leishmania*-loaded GM-BM alone. Similarly, SHP-1 inhibition during DC vaccination increased the frequencies of IFN- $\gamma$ -producing CD4<sup>+</sup> T cells, without affecting cells producing only TNF- $\alpha$  (Figure S4B) or IL-4 production

(F and G) GM-BM (F) or Flt3L BMDCs (G) of the indicated genotype were exposed to titrated RAW cells treated with UV 16 h before (RAW-UV) or RAW cells infected with VACV-OVA not treated (RAW-VACV-OVA) or treated with UV (RAW-VACV-OVA-UV) to inactivate the virus. Where indicated, cells were treated for 30 min with NSC-87877 before adding the antigens. Cells were thereafter co-cultured for 6 h, in the presence of BFA for the last 4 h, with *in vitro* expanded OT-I T cells. Cultures were stained for CD8 and intracellular IFN- $\gamma$ . Production of IFN- $\gamma$  as mean  $\pm$  SEM from two pooled experiments is shown.

\*p < 0.05, \*\*p < 0.01, and \*\*\*p < 0.001 (unpaired two-tailed Student's t test in B, C, and E; one-way ANOVA with Tukey post hoc test in D, F, and G).

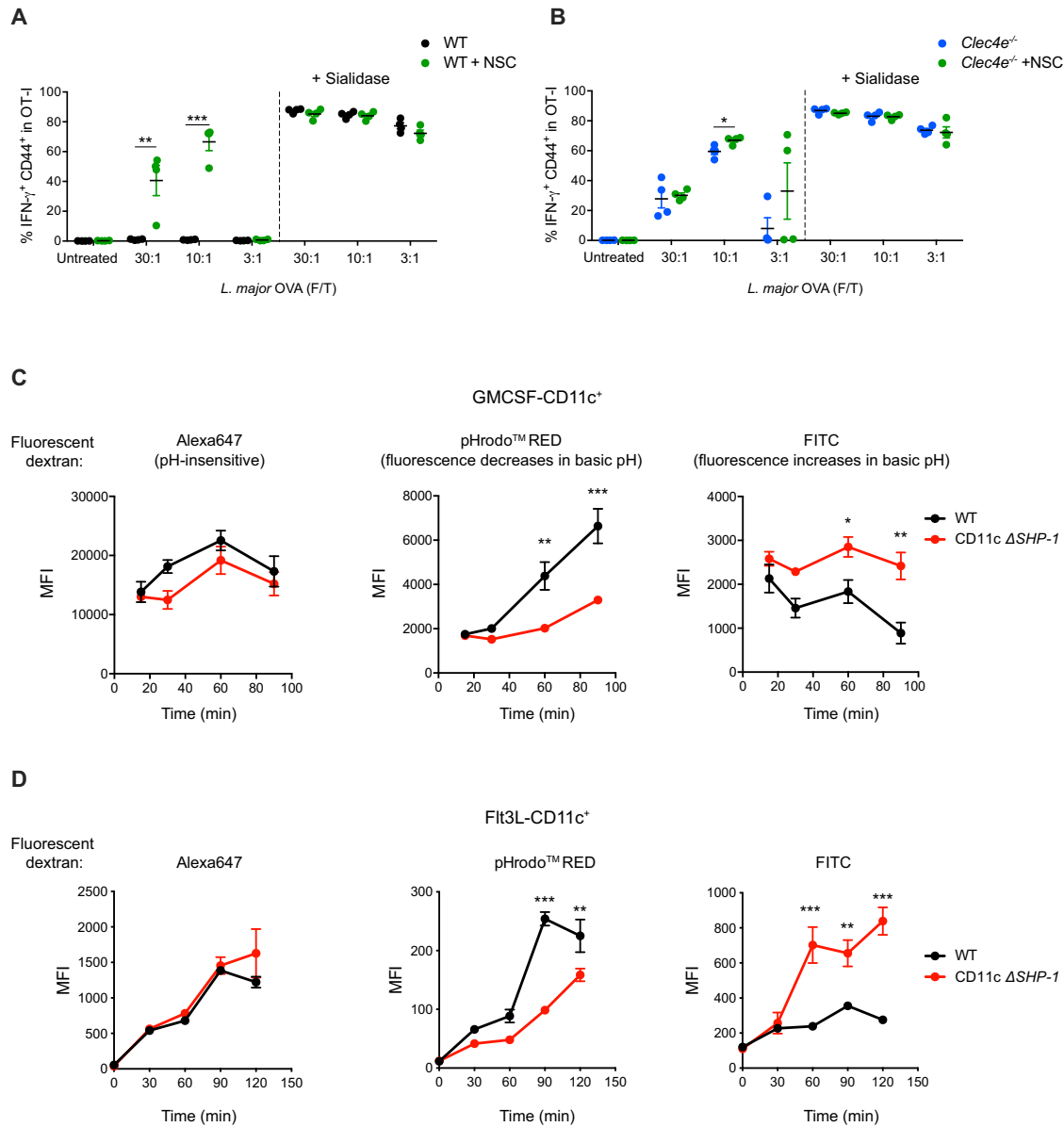


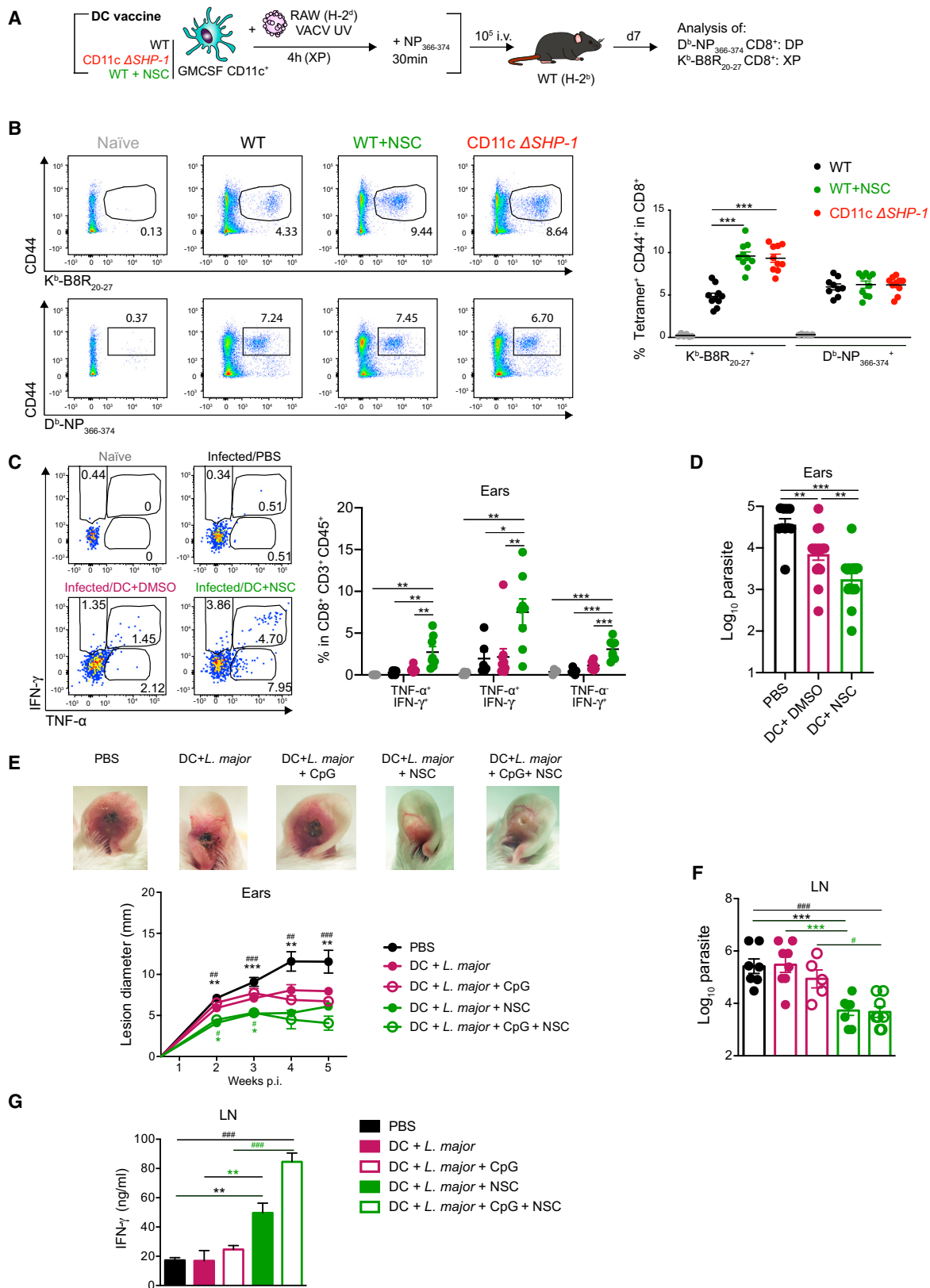
**Figure 3. SHP-1 Inhibition or Removal of Sialic Acid Adsorbed to the Parasite Boosts the Cross-Presentation Ability of Antigen-Presenting Cells**

(A and B) Removal of sialic acid adsorbed to *L. major* increases antigen cross-presentation in both WT and Mincle-deficient GM-BM. CD11c<sup>+</sup> cells were purified from GM-BM of the indicated genotype and exposed for 4 h to titrated F/T *L. major*-OVA extracts pretreated or not with sialidase for 1 h (neuraminidase, 0.1 U/mL). Where indicated, cells were treated for 30 min with NSC-87877, before adding the antigens. Thereafter, cells were co-cultured for 6 h, in the presence of BFA for the last 4 h, with *in vitro* expanded OT-I T cells. Cultures were stained for CD8 and intracellular IFN- $\gamma$ . Production of IFN- $\gamma$  as mean  $\pm$  SEM from two pooled experiments is shown.

(C and D) SHP-1 promotes endosomal acidification. CD11c<sup>+</sup> cells purified from GM-BM (C) or Flt3L BMDCs (D) were pulsed with 50  $\mu$ g/mL of the indicated dextran and during the indicated time. Graph shows mean fluorescence intensity (MFI)  $\pm$  SEM data from a representative experiment out of three performed. \* $p < 0.05$ , \*\* $p < 0.01$ , \*\*\* $p < 0.001$  (Student's t test in A and B; one-way repeated-measures ANOVA with Bonferroni post hoc test in C and D).

(Figure S4C). A single inoculation of SHP-1 inhibited GM-BM loaded with *Leishmania* antigens significantly reduced the inflammation of the ear, compared with vaccination with non-inhibited GM-BM treated with CpG ODN or not (Figure 4E). Moreover, only mice vaccinated with NSC-87877-treated DCs

showed lower parasite loads in the auricular dLNs 5 weeks after infection compared with controls (Figure 4F), independently of the adjuvant, and correlating with increased secretion of IFN- $\gamma$  in the supernatants of antigen-stimulated dLN cell cultures (Figure 4G). Interestingly, we found some decrease in



(legend on next page)



the ear lesions caused by *L. major* infection in mice inoculated with DMSO-treated GM-BM compared with PBS controls (Figure 4E) and in the parasite load in the skin (Figure 4D), but not in the dLNs (Figure 4F). This protection might be mediated by TNF- $\alpha$ <sup>+</sup> CD4<sup>+</sup> T cells in the skin, as we only found parasite-specific IFN- $\gamma$  production in the dLNs (Figure 4G) and in the skin (Figure 4C) when SHP-1 was inhibited.

Globally, we describe here that *Leishmania* inhibits cross-presentation in DCs via SHP-1 to evade CD8<sup>+</sup> T cells responses. These effects are partially mediated by Mincle (Iborra et al., 2016a; Martínez-López et al., 2019) but also by other receptors signaling through SHP-1 phosphatase activation. In line with a previous report (Ding et al., 2016), our results indicate that sialic acid recognition is one of these SHP-1-mediated mechanisms involved in inhibiting antigen cross-presentation. These results might be relevant for immune homeostasis and might partially explain the autoimmune responses observed in CD11c $\Delta$ SHP-1 mice (Abram and Lowell, 2017; Abram et al., 2013; Kaneko et al., 2012) or the autoimmune disorders associated to sialic acid recognition (reviewed by Mahajan and Pillai, 2016). Similarly, part of the CD8<sup>+</sup> T cell-associated beneficial effects of sialic acid blockade in tumors (Büll et al., 2018), or inhibiting SHP-1 during DC immunotherapy (Ramachandran et al., 2011), might be related to increased cross-presentation (Silva et al., 2016).

## STAR★METHODS

Detailed methods are provided in the online version of this paper and include the following:

- KEY RESOURCES TABLE
- RESOURCE AVAILABILITY
  - Lead contact
  - Materials Availability
  - Data and Code Availability
- EXPERIMENTAL MODEL AND SUBJECT DETAILS
  - Experimental Animals
  - Microbe strains
- METHOD DETAILS

- Parasite preparation and antigen extracts
- Sialic acid detection by flow cytometry on parasites and GM-BM CD11c<sup>+</sup> cells
- Viral infection and UV irradiation of RAW cells
- Mouse cell isolation, T cell activation and restimulation
- Flow cytometry
- Cell purification and adoptive transfer experiments
- GM-CSF and Flt3L Bone Marrow-derived cells generation
- *In vitro* analysis of antigen presentation
- DC vaccination

## ● QUANTIFICATION AND STATISTICAL ANALYSIS

## SUPPLEMENTAL INFORMATION

Supplemental Information can be found online at <https://doi.org/10.1016/j.celrep.2020.108468>.

## ACKNOWLEDGMENTS

We are grateful to Clifford Lowell, the David Sancho laboratory, and the Immunology Department at Universidad Complutense de Madrid (UCM) for discussions and critical reading of the manuscript. We thank the Centro Nacional de Investigaciones Cardiovasculares Carlos III (CNIC) and UCM facilities. We are indebted to D. Sancho, C. Lowell, C. Wells, R. Ashman, J. Yewdell, D. Sacks, P. Kaye, and D. Smith for providing critical reagents. Work in the S.I. laboratory is funded by the Spanish Ministerio de Ciencia e Innovación (MICINN), Agencia Estatal de Investigación, and Fondo Europeo de Desarrollo Regional (RTI2018-094484-B-I00 and RYC-2016-19463). S.C.K. is a recipient of a FPU fellowship (FPU16/03142) from the Spanish Ministry of Education, Culture and Sports. M.M.-L. is a recipient of an EMBO Long-Term Fellowship (EMBO LTF 463-2019).

## AUTHOR CONTRIBUTIONS

S.C.K., E.C.L.C., E.H.-G., M.M.-L., R.C.-G., and S.I. did the experiments. S.C.K., E.C.L.C., and S.I. conceived and designed experiments, analyzed data, and wrote the manuscript. All authors discussed the results and the manuscript.

## DECLARATION OF INTERESTS

The authors declare no competing interests.

## Figure 4. SHP-1 Inhibition Improves GM-BM Vaccination and Promotes Protection to *L. major* Challenge

(A and B) SHP-1 inhibition improves cross-priming of CD8<sup>+</sup> T cells upon GM-BM immunization. (A) Scheme of DC vaccine generation. WT GM-BM, treated or not with NSC-87877, or SHP-1-deficient GM-BM were exposed for 4 h to RAW cells infected with VACV and treated with UV 16 h before (RAW-VACV-UV) to inactivate the virus (ratio 1:1). Next, GM-BM were additionally loaded with an excess of NP<sub>366-374</sub> peptide for 30 min and inoculated i.v. into mice. (B) Left: representative plots of CD44<sup>+</sup> K<sup>b</sup>-B8R<sub>20-27</sub> tetramer<sup>+</sup> or CD44<sup>+</sup>D<sup>b</sup>-NP<sub>366-374</sub> tetramer<sup>+</sup> in the spleen, 7 days after inoculation. Right: frequencies of CD44<sup>+</sup>K<sup>b</sup>-B8R<sub>20-27</sub> tetramer<sup>+</sup> or CD44<sup>+</sup>D<sup>b</sup>-NP<sub>366-374</sub> tetramer<sup>+</sup> in CD8<sup>+</sup> T cells in the spleen.

(C–G) SHP-1 inhibition during vaccination with *Leishmania*-loaded GM-BM protects BALB/c mice against *L. major* infection. CD11c<sup>+</sup> cells purified from WT GM-BM were exposed for 4 h to *L. major* V1 F/T extracts (1:1 ratio) together or not with CpG (20  $\mu$ g/mL). Where indicated, cells were treated for 30 min with NSC-87877, before adding the antigens. Treated GM-BM (10<sup>6</sup>) were inoculated i.d. in the ears of BALB/c mice. At 6 weeks after vaccination, mice were challenged i.d. with 5  $\times$  10<sup>3</sup> *L. major* V1 parasites. (C and D) Ear cell suspensions from the indicated mice were obtained at day 6 p.i. (C) Ear cells were co-cultured with GM-BM loaded with *L. major* V1 F/T for 6 h, in the presence of BFA for the last 4 h. Cells were stained for CD45, CD3, and CD8 and intracellular IFN- $\gamma$  and TNF- $\alpha$ . Left: representative dot plot. Right: quantification of the percentages of IFN- $\gamma$ <sup>+</sup>, TNF- $\alpha$ <sup>+</sup>, or double-positive CD8<sup>+</sup> T cells. (D) Parasite load in the infected ears at day 6 p.i. (E) Upper panel: representative images of ear lesions at 5 weeks p.i. Lower panel: lesion diameter was monitored weekly after infection with a digital caliper. (F and G) At 5 weeks p.i., dLNs of the infected ears were harvested for quantification of the parasite load (F) and measurement of IFN- $\gamma$  production following restimulation with *L. major* V1 F/T extracts (G).

In (B), individual data from two independent experiments are shown as mean  $\pm$  SEM. In (C) and (D), individual data from a representative experiment of two performed are shown as mean  $\pm$  SEM. In (E)–(G), individual data from a representative experiment of two performed are shown as mean  $\pm$  SEM. Black asterisks: comparison between PBS and DC + *L. major* + NSC; black pound signs: comparison between PBS and DC + *L. major* + NSC + CpG; green asterisks: comparison between DC + *L. major*  $\pm$  NSC; green pound signs: comparison between DC + *L. major* + CpG  $\pm$  NSC. In (A)–(G), one-way ANOVA with Tukey post hoc test.\* p < 0.05; \*\* p < 0.01; \*\*\* p < 0.001.

Received: June 25, 2020  
Revised: October 15, 2020  
Accepted: November 10, 2020  
Published: December 1, 2020

## REFERENCES

- Abram, C.L., and Lowell, C.A. (2017). Shp1 function in myeloid cells. *J. Leukoc. Biol.* *102*, 657–675.
- Abram, C.L., Roberge, G.L., Pao, L.I., Neel, B.G., and Lowell, C.A. (2013). Distinct roles for neutrophils and dendritic cells in inflammation and autoimmunity in motheaten mice. *Immunity* *38*, 489–501.
- Belkaid, Y., Von Stebut, E., Mendez, S., Lira, R., Caler, E., Bertholet, S., Udey, M.C., and Sacks, D. (2002). CD8+ T cells are required for primary immunity in C57BL/6 mice following low-dose, intradermal challenge with *Leishmania major*. *J. Immunol.* *168*, 3992–4000.
- Bertholet, S., Debrabant, A., Afrin, F., Caler, E., Mendez, S., Tabbara, K.S., Belkaid, Y., and Sacks, D.L. (2005). Antigen requirements for efficient priming of CD8+ T cells by *Leishmania major*-infected dendritic cells. *Infect. Immun.* *73*, 6620–6628.
- Bertholet, S., Goldszmid, R., Morrot, A., Debrabant, A., Afrin, F., Collazo-Custodio, C., Houde, M., Desjardins, M., Sher, A., and Sacks, D. (2006). *Leishmania* antigens are presented to CD8+ T cells by a transporter associated with antigen processing-independent pathway in vitro and in vivo. *J. Immunol.* *177*, 3525–3533.
- Boussoffara, T., Boubaker, M.S., Ben Ahmed, M., Mokni, M., Feriani, S., Ben Salah, A., and Louzir, H. (2019). Activated cytotoxic T cells within zoonotic cutaneous leishmaniasis lesions. *Immun. Inflamm. Dis.* *7*, 95–104.
- Büll, C., Boltje, T.J., Balneger, N., Weischer, S.M., Wassink, M., van Germet, J.J., Bloemendal, V.R., Boon, L., van der Vlag, J., Heise, T., et al. (2018). Sialic acid blockade suppresses tumor growth by enhancing T-cell-mediated tumor immunity. *Cancer Res.* *78*, 3574–3588.
- Chava, A.K., Chatterjee, M., Gerwig, G.J., Kamerling, J.P., and Mandal, C. (2004). Identification of sialic acids on *Leishmania donovani* amastigotes. *Biol. Chem.* *385*, 59–66.
- Ding, Y., Guo, Z., Liu, Y., Li, X., Zhang, Q., Xu, X., Gu, Y., Zhang, Y., Zhao, D., and Cao, X. (2016). The lectin Siglec-G inhibits dendritic cell cross-presentation by impairing MHC class I-peptide complex formation. *Nat. Immunol.* *17*, 1167–1175.
- Enamorado, M., Iborra, S., Priego, E., Cueto, F.J., Quintana, J.A., Martínez-Cano, S., Mejías-Pérez, E., Esteban, M., Melero, I., Hidalgo, A., et al. (2017). Enhanced anti-tumour immunity requires the interplay between resident and circulating memory CD8(+) T cells. *Nat. Commun.* *8*, 16073.
- Gautam, S., Kumar, R., Singh, N., Singh, A.K., Rai, M., Sacks, D., Sundar, S., and Nylén, S. (2014). CD8 T cell exhaustion in human visceral leishmaniasis. *J. Infect. Dis.* *209*, 290–299.
- Helft, J., Böttcher, J., Chakravarty, P., Zelenay, S., Huotari, J., Schraml, B.U., Goubau, D., and Reis e Sousa, C. (2015). GM-CSF mouse bone marrow cultures comprise a heterogeneous population of CD11c(+)MHCII(+) macrophages and dendritic cells. *Immunity* *42*, 1197–1211.
- Hildner, K., Edelson, B.T., Purtha, W.E., Diamond, M., Matsushita, H., Kohyama, M., Calderon, B., Schraml, B.U., Unanue, E.R., Diamond, M.S., et al. (2008). Batf3 deficiency reveals a critical role for CD8α+ dendritic cells in cytotoxic T cell immunity. *Science* *322*, 1097–1100.
- Huster, K.M., Koffler, M., Stemberger, C., Schiemann, M., Wagner, H., and Busch, D.H. (2006). Unidirectional development of CD8+ central memory T cells into protective *Listeria*-specific effector memory T cells. *Eur. J. Immunol.* *36*, 1453–1464.
- Iborra, S., Izquierdo, H.M., Martínez-López, M., Blanco-Menéndez, N., Reis e Sousa, C., and Sancho, D. (2012). The DC receptor DNGR-1 mediates cross-priming of CTLs during vaccinia virus infection in mice. *J. Clin. Invest.* *122*, 1628–1643.
- Iborra, S., Martínez-López, M., Cueto, F.J., Conde-Garrosa, R., Del Fresno, C., Izquierdo, H.M., Abram, C.L., Mori, D., Campos-Martín, Y., Reguera, R.M., et al. (2016a). *Leishmania* uses Mincle to target an inhibitory ITAM signaling pathway in dendritic cells that dampens adaptive immunity to infection. *Immunity* *45*, 788–801.
- Iborra, S., Martínez-López, M., Khouili, S.C., Enamorado, M., Cueto, F.J., Conde-Garrosa, R., Del Fresno, C., and Sancho, D. (2016b). Optimal generation of tissue-resident but not circulating memory T cells during viral infection requires crosspriming by DNGR-1+ dendritic cells. *Immunity* *45*, 847–860.
- Kaneko, T., Saito, Y., Kotani, T., Okazawa, H., Iwamura, H., Sato-Hashimoto, M., Kanazawa, Y., Takahashi, S., Hiromura, K., Kusakari, S., et al. (2012). Dendritic cell-specific ablation of the protein tyrosine phosphatase Shp1 promotes Th1 cell differentiation and induces autoimmunity. *J. Immunol.* *188*, 5397–5407.
- Kim, T.S., Gorski, S.A., Hahn, S., Murphy, K.M., and Braciale, T.J. (2014). Distinct dendritic cell subsets dictate the fate decision between effector and memory CD8(+) T cell differentiation by a CD24-dependent mechanism. *Immunity* *40*, 400–413.
- Klebanoff, C.A., Gattinoni, L., and Restifo, N.P. (2006). CD8+ T-cell memory in tumor immunology and immunotherapy. *Immunol. Rev.* *211*, 214–224.
- Mahajan, V.S., and Pillai, S. (2016). Sialic acids and autoimmune disease. *Immunol. Rev.* *269*, 145–161.
- Mantegazza, A.R., Savina, A., Vermeulen, M., Pérez, L., Geffner, J., Hermine, O., Rosenzweig, S.D., Faure, F., and Amigorena, S. (2008). NADPH oxidase controls phagosomal pH and antigen cross-presentation in human dendritic cells. *Blood* *112*, 4712–4722.
- Martínez-López, M., Iborra, S., Conde-Garrosa, R., and Sancho, D. (2015). Batf3-dependent CD103+ dendritic cells are major producers of IL-12 that drive local Th1 immunity against *Leishmania major* infection in mice. *Eur. J. Immunol.* *45*, 119–129.
- Martínez-López, M., Soto, M., Iborra, S., and Sancho, D. (2018). *Leishmania* Hijacks Myeloid Cells for Immune Escape. *Front. Microbiol.* *9*, 883.
- Martínez-López, M., Iborra, S., Conde-Garrosa, R., Mastrangelo, A., Danne, C., Mann, E.R., Reid, D.M., Gaboriau-Routhiau, V., Chaparro, M., Lorenzo, M.P., et al. (2019). Microbiota sensing by Mincle-Syk axis in dendritic cells regulates interleukin-17 and -22 production and promotes intestinal barrier integrity. *Immunity* *50*, 446–461.e9.
- Matheoud, D., Moradin, N., Bellemare-Pelletier, A., Shio, M.T., Hong, W.J., Olivier, M., Gagnon, É., Desjardins, M., and Descoteaux, A. (2013). *Leishmania* evades host immunity by inhibiting antigen cross-presentation through direct cleavage of the SNARE VAMP8. *Cell Host Microbe* *14*, 15–25.
- Matte, C., Casgrain, P.A., Séguin, O., Moradin, N., Hong, W.J., and Descoteaux, A. (2016). *Leishmania major* promastigotes evade LC3-associated phagocytosis through the action of GP63. *PLoS Pathog.* *12*, e1005690.
- Medina, F., Ramos, M., Iborra, S., de León, P., Rodríguez-Castro, M., and Del Val, M. (2009). Furin-processed antigens targeted to the secretory route elicit functional TAP1-/-CD8+ T lymphocytes in vivo. *J. Immunol.* *183*, 4639–4647.
- Nateghi Rostami, M., Keshavarz, H., Edalat, R., Sarrafnejad, A., Shahrestani, T., Mahboudi, F., and Khamesipour, A. (2010). CD8+ T cells as a source of IFN-γ production in human cutaneous leishmaniasis. *PLoS Negl. Trop. Dis.* *4*, e845.
- Prickett, Sara, et al. (2006). In Vivo Recognition of Ovalbumin Expressed by Transgenic *Leishmania* Is Determined by Its Subcellular Localization. *The Journal of Immunology*. <https://doi.org/10.4049/jimmunol.176.8.4826>.
- Ramachandran, I.R., Song, W., Lapteva, N., Seethamagari, M., Slawin, K.M., Spencer, D.M., and Levitt, J.M. (2011). The phosphatase SRC homology region 2 domain-containing phosphatase-1 is an intrinsic central regulator of dendritic cell function. *J. Immunol.* *186*, 3934–3945.
- Ribeiro-Gomes, F.L., Romano, A., Lee, S., Roffé, E., Peters, N.C., Debrabant, A., and Sacks, D. (2015). Apoptotic cell clearance of *Leishmania major*-infected neutrophils by dendritic cells inhibits CD8+ T-cell priming in vitro by Mer tyrosine kinase-dependent signaling. *Cell Death Dis.* *6*, e2018.
- Roy, S., and Mandal, C. (2016). *Leishmania donovani* utilize sialic acids for binding and phagocytosis in the macrophages through selective utilization

- of Siglecs and impair the innate immune arm. *PLoS Negl. Trop. Dis.* **10**, e0004904.
- Savina, A., Jancic, C., Hugues, S., Guernonprez, P., Vargas, P., Moura, I.C., Lennon-Duménil, A.-M., Seabra, M.C., Raposo, G., and Amigorena, S. (2006). NOX2 controls phagosomal pH to regulate antigen processing during crosspresentation by dendritic cells. *Cell* **126**, 205–218.
- Schmidt, M.E., and Varga, S.M. (2018). The CD8 T cell response to respiratory virus infections. *Front. Immunol.* **9**, 678.
- Silva, M., Silva, Z., Marques, G., Ferro, T., Gonçalves, M., Monteiro, M., van Vliet, S.J., Mohr, E., Lino, A.C., Fernandes, A.R., et al. (2016). Sialic acid removal from dendritic cells improves antigen cross-presentation and boosts anti-tumor immune responses. *Oncotarget* **7**, 41053–41066.
- Silva, Z., Ferro, T., Almeida, D., Soares, H., Ferreira, J.A., Deschepper, F.M., Hensbergen, P.J., Pirro, M., van Vliet, S.J., Springer, S., and Videira, P.A. (2020). MHC class I stability is modulated by cell surface sialylation in human dendritic cells. *Pharmaceutics* **12**, 249.
- Stäger, S., and Rafati, S. (2012). CD8(+) T cells in leishmania infections: friends or foes? *Front. Immunol.* **3**, 5.
- Uzonna, J.E., Joyce, K.L., and Scott, P. (2004). Low dose Leishmania major promotes a transient T helper cell type 2 response that is down-regulated by interferon gamma-producing CD8+ T cells. *J. Exp. Med.* **199**, 1559–1566.
- Viana, A.G., Magalhães, L.M.D., Giunchetti, R.C., Dutra, W.O., and Gollob, K.J. (2019). Leishmania infantum induces expression of the negative regulatory checkpoint, CTLA-4, by human naïve CD8<sup>+</sup> T cells. *Parasite Immunol.* **41**, e12659.
- Wells, C.A., Salvage-Jones, J.A., Li, X., Hitchens, K., Butcher, S., Murray, R.Z., Beckhouse, A.G., Lo, Y.-L.-S., Manzanero, S., Cobbold, C., et al. (2008). The macrophage-inducible C-type lectin, mincle, is an essential component of the innate immune response to *Candida albicans*. *J. Immunol.* **180**, 7404–7413.
- Wherry, E.J., and Ahmed, R. (2004). Memory CD8 T-cell differentiation during viral infection. *J. Virol.* **78**, 5535–5545.
- Yewdell, J.W., Dersh, D., and Fähræus, R. (2019). Peptide channeling: the key to MHC class I immunosurveillance? *Trends Cell Biol.* **29**, 929–939.
- Zammit, D.J., Cauley, L.S., Pham, Q.-M., and Lefrançois, L. (2005). Dendritic cells maximize the memory CD8 T cell response to infection. *Immunity* **22**, 561–570.
- Zelenay, S., Keller, A.M., Whitney, P.G., Schraml, B.U., Deddouche, S., Rogers, N.C., Schulz, O., Sancho, D., and Reis e Sousa, C. (2012). The dendritic cell receptor DNGR-1 controls endocytic handling of necrotic cell antigens to favor cross-priming of CTLs in virus-infected mice. *J. Clin. Invest.* **122**, 1615–1627.

STAR★METHODS

KEY RESOURCES TABLE

REAGENT or RESOURCE	SOURCE	IDENTIFIER
Antibodies		
anti-mouse CD45.1, APC, clone A20	eBiosciences	Cat# 17-0453-81; RRID:AB_469397
anti-mouse CD45.1, PerCP-Cyanine5.5, clone A20	eBiosciences	Cat# 45-0453-82; RRID:AB_1107003
anti-mouse CD45.1, eFluor 450, clone A20	eBiosciences	Cat# 48-0453-82; RRID:AB_1272189
anti-mouse CD45, eFluor 450, clone 30-F11	eBiosciences	Cat# 48-0451-82; RRID:AB_1518806
anti-mouse CD45.1, V450, clone A20	BD Biosciences	Cat# 560520; RRID:AB_1727490
anti-mouse CD16/CD32, clone 2.4G2	Tonbo	Cat# 70-0161; RRID:AB_2621487
anti-mouse CD44, FITC, clone IM7	eBiosciences	Cat# 11-0441-81; RRID:AB_465044
anti-mouse CD44, v450, clone IM7	BD Biosciences	Cat# 560452; RRID:AB_1645274
anti-mouse CD3e, FITC, clone 145-2C11	Tonbo	Cat# 35-0031; RRID:AB_2621659
anti-mouse CD4, PE, clone GK1.5	Tonbo	Cat# 50-0041; RRID:AB_2621736
anti-mouse CD8a, PerCP-Cy5.5, clone 53-6.7	Tonbo	Cat# 65-0081; RRID:AB_2621882
anti-mouse CD8a, PE, clone 53-6.7	eBiosciences	Cat# 12-0081-83; RRID:AB_465531
anti-mouse CD11b, APC, clone M1/70	eBiosciences	Cat# 17-0112-83; RRID:AB_469344
anti-mouse IFN- $\gamma$ , APC, clone XMG1.2	eBiosciences	Cat# 17-7311-82; RRID:AB_469504
anti-mouse TNF- $\alpha$ , Antibody PE, clone MP6-XT22	BioLegend	Cat# 506306; RRID: AB_315427
anti-mouse IFN- $\gamma$ , APCy7, clone XMG1.2	BioLegend	Cat# 505849; RRID:AB_2616697
anti-mouse I-A/I-E (MHCII), FITC, clone 2G9	BD Biosciences	Cat# 553623; RRID:AB_394958
anti-mouse CD4, APC, clone RM4-5	BD Biosciences	Cat# 553051; RRID:AB_398528
anti-mouse CD4, PerCP-Cy5.5, clone RM4-5	BD Biosciences	Cat# 550954; RRID:AB_393977
anti-mouse CD11c, APC, clone HL3	BD Biosciences	Cat# 550261; RRID:AB_398460
anti-mouse CD11c, PE, clone HL3	BD Biosciences	Cat# 553802; RRID:AB_395061
anti-mouse CD45R/B220, BV421, clone RA3-6B2	BD Bioscience	Cat# 562922, RRID:AB_2737894
anti-mouse CD11b, FITC, clone M1/70	BD Biosciences	Cat# 11-0112-85; RRID:AB_464936
anti-mouse I-A/I-E (MHCII), AF700, clone M5/114.15.2	BioLegend	Cat# 107621; RRID:AB_493726
anti-mouse/human CD11b, BV605, clone M1/70	BioLegend	Cat# 101237; RRID:AB_11126744
anti-mouse/human CD11b, APCFire750, clone M1/70	BioLegend	Cat# 101262; RRID:AB_2572122
anti-mouse/rat XCR1, PE, clone ZET	BioLegend	Cat# 148204; RRID:AB_2563843
anti-mouse CD172a (SIRP $\alpha$ ), PerCP/Cy5.5, clone P84	BioLegend	Cat# 144009; RRID:AB_2563547
anti-mouse CD4, PECy7, clone RM4-5	BioLegend	Cat# 100528; RRID:AB_312729
anti-mouse/human CD11b, APC/Cy7, clone M1/70	BioLegend	Cat# 101226; RRID:AB_830642
anti-mouse CD11c, Biotin Conjugated, Clone HL3	BD Bioscience	Cat# 553800; RRID:AB_395059
anti-mouse/human CD11b, Biotin Conjugated, Clone M1/70	BD Bioscience	Cat# 553309; RRID:AB_394773
anti-mouse/human CD45R/B220, Biotin Conjugated, Clone RA3-6B2	BD Bioscience	Cat# 553086; RRID:AB_394616
anti-mouse I-A/I-E (MHCII), Biotin Conjugated, Clone 2G9	BD Bioscience	Cat# 553622; RRID:AB_394957
anti-mouse CD4, Biotin Conjugated, Clone GK1.5	BD Bioscience	Cat# 553728; RRID:AB_395012
anti-mouse Ly-6G, Ly-6C, Biotin Conjugated, Clone RB6-8C5	BD Bioscience	5Cat# 553124; RRID:AB_394640
anti-mouse CD16/32, Biotin Conjugated, Clone 2.4G2	BD Bioscience	Cat# 553143, RRID:AB_394658
anti-mouse CD370 (CLEC9A, DNGR1) APC	BioLegend	Cat# 143505; RRID: AB_2566379
Anti-mouse CD24 (eBioSN3 (SN3 A5-2H10)), PE	eBiosciences	Cat# 12-0247-42 RRID: AB_1548678

(Continued on next page)

**Continued**

REAGENT or RESOURCE	SOURCE	IDENTIFIER
<b>Bacterial and Virus Strains</b>		
<i>Leishmania major</i> Friedlin clone V1 (FV1) (MHOM/IL/80/Friedlin)	Isolated from a patient with localized cutaneous leishmaniasis in Israel. David Sacks (NIAID, NIH, USA)	N/A
<i>L. major</i> Friedlin clone VI expressing OVA (PHOC <i>L. major</i> )	(Prickett, 2006) Paul M. Kaye and Deborah F. Smith (University of York, UK)	N/A
Vaccinia virus WR	Jonathan W. Yewdell and Jack R. Bennink (National Institutes of Health, Bethesda, MD)	N/A
<b>Chemicals, Peptides, and Recombinant Proteins</b>		
Liberase TL Research Grade	Roche	Cat# 5401020001
DNase I, Bovine Pancreas, > 2000U/MG	Biomatik	Cat# A4193
Neuraminidase (Sialidase)	Sigma	Cat# 10269611001
SHP-1/2 PTPase inhibitor NSC-87877	Merk Millipore	Cat# 565851-50MG
Sodium Stibogluconate	Merk Millipore	Cat# 567565-1GM
CpG ODN1826	Invivogen	Cat# tlr1-1826-1
OVA <sup>257</sup> SIINFEKL <sup>264</sup> peptide	GeneScript	N/A
B8R <sup>(20TSYKFESV<sup>27</sup>)</sup> peptide	GeneScript	N/A
NP <sup>(366ASNMMDAM<sup>374</sup>)</sup> peptide	GeneScript	N/A
VACV, H-2Kb <sup>(20TSYKFESV<sup>27</sup>, B8R)</sup> tetramer	NIH Tetramer Facility at Emory University	N/A
OVA H-2Kb <sup>(257SIINFEKL<sup>264</sup>)</sup> dextramer	Immudex	Cat# JD2163
Influenza PR8, H-2Db <sup>(366ASNMMDAM<sup>374</sup>, NP)</sup> tetramer	NIH Tetramer Facility at Emory University	N/A
CellTrace Violet Cell Proliferation Kit	Invitrogen	Cat# C34557
Recombinant murine GM-CSF	Miltenyi Biotec	Cat# 130-095-746
Mouse Flt3L, research grade	Miltenyi Biotec	Cat# 130-097-372
Human IL-2 IS research grade	Miltenyi Biotec	Cat# 130-097-743
Streptavidin APC	eBioscience	Cat# 17-4317-82
Streptavidin PE	eBioscience	Cat# 12-4317-87
Streptavidin PerCP-Cyanine5.5	eBioscience	Cat# 45-4317-82
LIVE/DEAD Fixable Near-IR Dead Cell Stain Kit	Molecular Probes	Cat# 10154363
Hoechst 33258	ThermoFisher	Cat# H3569; RRID:AB_2651133
SureBlue TMB 1- Peroxidase Substrate	SeraCare	Cat# 5120-0075
TMB Stop Solution	SeraCare	Cat# 5150-0020
Fluorescein isothiocyanate-dextran	Sigma-Aldrich	Cat# 46944
Dextran, Alexa Fluor 647; 10,000 MW, Anionic, Fixable	Thermofisher	Cat# D22914
pHrodo Red Dextran, 10,000 MW, for Endocytosis	Thermofisher	Cat# P10361
Recombinant Human Siglec 5-Fc Chimera (carrier-free)	Biolegend	Cat#557204
Recombinant human Clec4e (Mincle) Fc Chimera Protein	R&D Systems	Cat# 8995-CL-050
Recombinant Human IgG1 Fc, CF	R&D Systems	Cat#110-HG-100
Sambucus Nigra (Elderberry Bark) Lectin (SNA, EBL), fluorescein (FITC)	Thermofisher	Cat#L32479
<b>Critical Commercial Assays</b>		
Mouse IL-4 ELISA Set	BD Biosciences	Cat# 555232
Mouse IFN- $\gamma$ ELISA Set	BD Biosciences	Cat# 551866

(Continued on next page)

**Continued**

REAGENT or RESOURCE	SOURCE	IDENTIFIER
Experimental Models: Organisms/Strains		
Mouse: <i>Clec4e</i> <sup>-/-</sup> (B6.Cg-Clec4e <sup>tm1.1Ctg</sup> )	(Wells et al., 2008)	N/A
Mouse: CD11cΔ <i>SHP1</i> (B6.Cg-Tg(Itgax-cre)1-1Reiz/J <i>Ptpn6fl/fl</i> )	(Iborra et al., 2016a)	N/A
Mouse: OT-I (C57BL/6-Tg(TcraTcrb)1100Mjb/J)	Jackson Laboratory	Cat# 003831
Software and Algorithms		
FlowJo v10	Tree Star	<a href="https://www.flowjo.com/solutions/flowjo/downloads">https://www.flowjo.com/solutions/flowjo/downloads</a>
GraphPad Prism v8	GraphPad Software	N/A
Other		
Streptavidin MicroBeads	Miltenyi Biotec	Cat# 130-048-101
Anti-mouse CD11c MicroBeads	Miltenyi Biotec	Cat# 130-097-059
Brefeldin A	Sigma-Aldrich	Cat# B7651

**RESOURCE AVAILABILITY**

**Lead contact**

Further information and requests for resources and reagents should be directed to and will be fulfilled by the Lead Contact, Salvador Iborra ([siborra@ucm.es](mailto:siborra@ucm.es)).

**Materials Availability**

The mouse lines and parasites obtained from other laboratories may require a Material Transfer Agreement (MTA) with the providing scientists.

**Data and Code Availability**

This study did not generate/analyze [datasets/code].

**EXPERIMENTAL MODEL AND SUBJECT DETAILS**

**Experimental Animals**

Mice were bred and maintained in groups of 2-5 animals per cage at the CNIC under specific pathogen-free conditions. Males and females of 7-9 weeks old were used. Animal studies were approved by the local ethics committee. All animal procedures conformed to EU Directive 2010/63EU and Recommendation 2007/526/EC regarding the protection of animals used for experimental and other scientific purposes, enforced in Spanish law under Real Decreto 1201/2005.

*Clec4e*<sup>-/-</sup> (B6.Cg-Clec4e<sup>tm1.1Ctg</sup>) mice, backcrossed more than 10 times to C57BL/6J-Crl, were kindly provided by D. Sancho (CNIC) and originally provided by the Scripps Research Institute, through R. Ashman and C. Wells (Griffiths University, Australia) (Wells et al., 2008). CD11cΔ*SHP1* (Abram et al., 2013) and *Clec4e*<sup>-/-</sup> mice were generated along with WT littermates by heterozygous matings. OT-I CD8<sup>+</sup> TCR transgenic mice in C57BL/6 background (C57BL/6-Tg(TcraTcrb)1100Mjb/J) were from The Jackson Laboratory. OT-I mice were mated with B6/SJL expressing the CD45.1 congenic marker (The Jackson Laboratory) to facilitate cell tracking.

**Microbe strains**

*Leishmania major* Friedlin clone V1 (FV1) (MHOM/IL/80/Friedlin) was a kind gift from David Sacks (NIAID, NIH, Bethesda, USA) and *L. major* Friedlin clone VI expressing OVA (PHOC *L. major*) (Prickett et al., 2006) was generously provided by Paul M. Kaye and Deborah F. Smith (University of York, UK). The WR VACV strain was a kind gift from Jonathan W. Yewdell and Jack R. Bennink (National Institutes of Health, Bethesda, MD). Viral stocks were grown in CV-1 monolayers and used as clarified sonicated cell extracts (NIAID, NIH, Bethesda, USA).

**METHOD DETAILS**

**Parasite preparation and antigen extracts**

For *Leishmania* challenge, parasites of different lines were cultured and kept in a virulent state as described (Martínez-López et al., 2015). Mice were infected by i.d. inoculation of 10<sup>3</sup> (or 1 × 10<sup>5</sup> for *L. major*-OVA experiments) metacyclic *L. major* promastigotes into

the dermis of both ears (Martínez-López et al., 2015). Lesion size in the ear and number of viable parasites was determined as described (Martínez-López et al., 2015). The parasite load is expressed as the number of parasites in the whole organ. For preparation of Freeze-thawed (F/T) *L. major*, we performed 3 F/T cycles of  $10^8$  stationary parasites in complete RPMI medium [RPMI 1640 (GIBCO®) supplemented with 10% heat-inactivated fetal bovine serum, 50  $\mu$ M 2-mercaptoethanol (both Sigma), 2mM glutamine, 100 U/mL penicillin and 100  $\mu$ g/mL streptomycin (both Lonza), 0.1 mM NEAA, 1 mM Sodium Pyruvate, 1 mM HEPES (all from HyClone)]. Where indicated, *L. major* were pre-treated with Neuraminidase 0.1 U/mL (Sialidase; Sigma).

### Sialic acid detection by flow cytometry on parasites and GM-BM CD11c<sup>+</sup> cells

Freeze-thawed (F/T) *L. major* parasites were prepared by 3 cycles of freezing and thawing of  $10^7$  stationary parasites in complete RPMI medium from promastigotes grown in 20%, 5%, 2.5% FCS or Knockout Serum Replacement (GIBCO™). F/T promastigotes were stained in HBSS (with calcium) containing 2% skimmed milk, while GM-BM CD11c<sup>+</sup> cells were stained in HBSS + 2% FCS, with human Siglec 5-Fc chimera, human Clec4e-Fc chimera or hFc control (R&D Systems).

### Viral infection and UV irradiation of RAW cells

RAW264.7 macrophages (RAW cells) were grown in DMEM (GIBCO®) supplemented as above. RAW cells were irradiated with UVC (240 mJ/cm<sup>2</sup>) either without exposure to VACV (RAW UV) or after incubation with VACV for 4h (RAW-VACV-UV). Alternatively, infected RAW cells were left un-irradiated (RAW-VACV). RAW cells were used sixteen hours after UV irradiation for *in vitro* stimulation of GM-CSF BM-derived cells (GM-BM) and Flt3L-BMDC or injection into mice.

### Mouse cell isolation, T cell activation and restimulation

Peritoneal lavage was collected by injecting PBS into the peritoneal cavity. Ears were harvested in HBSS, ventral and dorsal sheets of the ears were separated, cut into small pieces and digested with Liberase/DNase in HBSS. After 30 min at 37°C, tissues were homogenized. Spleen and skin-draining lymph nodes were collected in RPMI complete medium and mechanically dissociated using tweezers and a syringe plunger. Tissue homogenates were filtered through a 70  $\mu$ m cell strainer (Falcon Products) and used for further analysis. To generate effector OT-I cells, splenocytes from OT-I mice were activated with 1nM SIINFEKL and 100 U/ml IL-2 (Miltenyi Biotec) in complete RPMI for 5 days. dLNs were plated at  $5 \times 10^6$  cells/well in p24 plates and restimulated with (F/T) *L. major* for 2 days. IFN- $\gamma$  and IL-4 production was measured by ELISA in culture supernatants with BD OptEIA ELISA kits according to the manufacturer's instructions. For analysis of intracellular cytokines, T cells were re-stimulated to induce cytokine production by incubation of cell suspensions with an excess of SIINFEKL or B8R peptide (1  $\mu$ M) for 6h, brefeldin A (Sigma, 5  $\mu$ g/ml) being added for the last 4h of culture.

### Flow cytometry

Samples for flow cytometry were stained in ice-cold PBS supplemented with 2.5% FBS, 2 mM EDTA. Cells were pre-incubated for 10 min at 4°C with anti-mouse CD16/CD32 (clone 2.4G2, Tonbo Bioscience) to block unspecific antibody binding before staining with the appropriate antibodies. For intracellular cytokine staining, after surface marker staining, cells were fixed in PFA 4% and intracellularly stained during permeabilization with 0.1% saponin. Anti-mouse antibodies to CD45.1 APC, CD45 efluor450, CD44 FITC, CD24 PE, CD8 $\alpha$  PE, CD11b APC, IFN- $\gamma$  APC were obtained from eBioscience. Anti-mouse I-A/I-E (MHCII) FITC, CD44 FITC, CD4 PerCP-Cy5.5, CD11c APC, CD45.1 V450, CD45R/B220 BV421, CD11b FITC, were from BD Biosciences. Anti-mouse I-A/I-E (MHCII) AF700, CD11b (APCFire750), XCR1 PE, CD172a (Sirp $\alpha$ ) PerCP-Cy5.5, CD4 TNF- $\alpha$  PE, b CD370 (CLEC9A, DNDR1) APC were from Biolegend. Anti-mouse CD8 $\alpha$  PerCP-Cy5.5, CD3 FITC was from Tonbo Biosciences. APC-labeled tetramers specific for VACV, H-2K<sup>b</sup> (<sup>20</sup>TSYKFESV<sup>27</sup>, B8R) and Influenza PR8, H-2Db (<sup>20</sup>ASNENMDAM<sup>27</sup>, NP) were provided by the NIH Tetramer Facility at Emory University. APC-labeled dextramers specific for OVA H-2K<sup>b</sup> (<sup>257</sup>SIINFEKL<sup>264</sup>) were purchased from Immudex. Non-cell permeant Hoechst 33258 (0.1  $\mu$ M, ThermoFisher) was used as a counterstain to detect murine necrotic cells. Data were acquired on an LSR Fortessa or in BD FACSymphony™ (BD Biosciences) and analyzed with FlowJo software version 10 (TreeStar).

### Cell purification and adoptive transfer experiments

Naive CD8<sup>+</sup> T cells were purified from spleen and lymph nodes cells of OT-I mice by negative selection using a cocktail of biotin-conjugated antibodies (anti-CD11c, CD11b, B220, MHC-II, CD4, GR1, CD16/32, BD Bioscience) and Streptavidin-microbeads (Miltenyi Biotec) followed by sorting based on expression of CD44 and CD62L using a FACs Aria cell sorter. Where indicated, cells were labeled with CellTrace Violet according to manufacturer's instructions (5  $\mu$ M, Thermo Fisher Scientific). CellTrace Violet-labeled purified CD8<sup>+</sup> OT-I T cells ( $10^5$ ) were transferred just after challenge in the ear dermis with  $10^5$  metacyclic promastigotes of *Leishmania*-OVA. 2.5 days post-infection (p.i.), dLNs were removed and CellTrace Violet dilution was analyzed by flow cytometry. In some experiments, CD8<sup>+</sup> T cells were purified by negative selection as described above from retromaxillary LNs of *L. major* V1 infected and healed mice or naive mice, enriched in CD44<sup>+</sup> cells by magnetic positive selection, labeled with CellTrace Violet and co-cultured with *L. major* V1 F/T-loaded GM-BM or Flt3L-BMDCs for 3 days. For purification of DC subsets from dLNs of *L. major* OVA infected mice, dLNs were digested with Liberase/DNase in HBSS and CD11c<sup>+</sup> cells enriched using anti-CD11c microbeads (Miltenyi Biotec) were further sorted into XCR1<sup>+</sup> CD11b<sup>-</sup> and XCR1<sup>-</sup> CD11b<sup>+</sup> migratory (CD11c<sup>+</sup> MHC class II<sup>hi</sup>) and resident (CD11c<sup>+</sup> MHC class II<sup>lo</sup>)

DCs using a FACSAria Sorter. Sorted DCs were co-cultured with effector OT-I and intracellular IFN- $\gamma$  was determined by flow cytometry.

### GM-CSF and Flt3L Bone Marrow-derived cells generation

Cell suspensions from bone marrow of the indicated genotypes were cultured in complete RPMI in tissue culture flasks (Falcon Products) in the presence of 20 ng/mL recombinant GM-CSF (Miltenyi Biotec). GM-BM were collected on day 8 and purified by positive selection with anti-CD11c-microbeads (Miltenyi Biotec). Mouse Flt3L-BMDCs were generated by culturing bone marrow cells in complete RPMI in the presence of 50 ng/ml Flt3L (R&D), adding medium on day 5. After 9 days, cells had a typical DC morphology, with approximately half of the cells exhibiting a CD8 $\alpha$ -like phenotype (MHC class II<sup>+</sup>, CD11c<sup>+</sup>, CD24<sup>hi</sup>, CD11b<sup>lo</sup>, B220<sup>-</sup>, DNGR-1<sup>+</sup>).

### In vitro analysis of antigen presentation

To test DC cross-presenting ability, CD11c<sup>+</sup> GM-BM or Flt3L-BMDCs were stimulated for 4h with serial dilutions of (F/T) *L. major* or by co-culture with VACV infected RAW cells treated or not with UV irradiation to inactivate the virus. To test the effect of SHP-1 inhibition on cross-presentation, antigen presenting cells were treated for 30 min before stimulation with either NSC-87877 (20  $\mu$ M, Merck Millipore) or Sodium Stibogluconate (SSG) (20  $\mu$ g/ml, Merk Millipore). Afterward, effector OT-I cells were added to the cultures for 6h, brefeldin A (Sigma, 5  $\mu$ g/ml) being added for the last 4h of culture. CD44<sup>+</sup> CD8<sup>+</sup> T cells enriched from *L. major* V1 infected and healed mice, as explained above, were co-cultured for 3 days with *L. major* V1 F/T-loaded Flt3L-BMDCs, and were further stimulated with PMA/ionomycin in the presence of brefeldin A for 4 hours. Cells were then stained for surface markers, fixed in 4% PFA and intracellularly stained for IFN- $\gamma$ . An average of 10,000 cells of each T cell subset were analyzed in each sample. To evaluate endosomal acidification, GM-BM and Flt3L-BMDCs were treated with Fluorescein isothiocyanate-dextran (Sigma), Alexa Fluor<sup>®</sup> 647 and pHrodo Red Dextran (both ThermoFisher), and fluorescence was analyzed by flow cytometry.

### DC vaccination

CD11c<sup>+</sup> GM-BM of the indicated genotype were treated for 30 min before stimulation with either NSC-87877 (20  $\mu$ M, Merck Millipore) or Sodium Stibogluconate (SSG) (20  $\mu$ g/ml, Merk Millipore), and stimulated with RAW-VACV-UV (1:1 ratio) for 4h. Cells were then loaded with the OVA<sub>257-264</sub> SIINFEKL peptide or NP<sub>366-374</sub> ASNENMDAM peptide for 30min. Cells were washed, and 10<sup>5</sup> cells were i.v. injected into WT C57BL/6 mice. 7 days after vaccination, induction of OVA-specific, NP-specific and B8R-specific CD8<sup>+</sup> T cells was assessed in the spleen. CD11c<sup>+</sup> GM-BM were pre-treated or not with NSC-87877 20  $\mu$ M for 30 min at 37°C. Cells were then stimulated with (F/T) *L. major* V1 (1:1 ratio) in combination or not with CpG ODN1826 (20  $\mu$ g/ml, Invivogen) for 4h. Cells were washed twice with PBS and 10<sup>6</sup> *Leishmania* pulsed GM-BM were i.d. injected in the ears of WT BALB/c mice. 6 weeks after vaccination, mice were challenged i.d. with live *L. major* V1 and lesion diameter was measured with a digital caliper. Ears were harvested 1 week p.i., to measure parasite load and cytokine production by CD8<sup>+</sup> T cells by flow cytometry. At week 5 p.i., ears and dLNs were harvested to quantify parasite load. dLNs were restimulated with (F/T) *L. major* for 2 days as described before and IFN- $\gamma$  and IL-4 production was measured by ELISA in culture supernatants with BD OptEIA ELISA kits.

### QUANTIFICATION AND STATISTICAL ANALYSIS

Statistical analysis was performed using GraphPad Prism 8 (GraphPad Software). Statistical significance for comparison between two sample groups with a normal distribution (Shapiro-Wilk test for normality), was determined by parametric Student's t test or one-way ANOVA with Tukey post hoc test unless otherwise stated. Differences with p values  $\leq$  0.05 were considered significant. \*, p < 0.05; \*\*, p < 0.01; \*\*\*, p < 0.001.